Supporting Information for:

Biohybrid Photosynthetic Antenna Complexes for Enhanced Light-Harvesting

Joseph W. Springer, Pamela S. Parkes-Loach, Kanumuri Ramesh Reddy,
Michael Krayer, Jieying Jiao, Gregory M. Lee,
Dariusz M. Niedzwiedzki, Michelle A. Harris, Christine Kirmaier,
David F. Bocian, Jonathan S. Lindsey, Dewey Holten and Paul A. Loach

Table of Contents

Additional Experimental Procedures

Preparation of Polypeptides with Covalently Attached Chromophores. The procedure followed was essentially that recommended by Invitrogen:Molecular Probes (Handbook of Fluorescent Probes and Research Products 2001) and is summarized here for conjugation of **BC2** to the 31mer(–14Cys) polypeptide. A sample of the polypeptide (3.0 mg) was dissolved in 230 µL of *N*,*N*-dimethylformamide (DMF), and 70 µL of 100 mM Tris buffer (pH 7.3) was added with stirring. A sample of **BC2** (2.0 mg) was dissolved in 230 µL of DMF, and 70 µL of 100 mM Tris buffer (pH 7.3) was added. This latter solution was slowly added to the former with stirring and under a gentle flow of Argon. The sample was stoppered and stirred for 2 h at room temperature in the dark. The reaction mixture was then dried under vacuum and stored at –20 °C. A portion of the dried material was dissolved in 35 µL of hexafluoroacetone trihydrate (HFA) to which was added 35 µL of 1:1 HPLC A:B solvent, and the sample injected into a Waters Breeze HPLC system with a Rheodyne manual injector and a Waters 2487 UV detector. Perkin-Elmer HCODS C18 columns (150 x 4.6 mm) were used for all purifications. The HPLC solvent system consisted of (A) 0.1% trifluoroacetic acid (TFA) as the aqueous solvent and (B) 0.1 % TFA in 2:1 (v/v) acetonitrile/2-propanol as the organic solvent.[24] Typical results are shown in Figure S-1. On the basis of extinction coefficients for **BC2** at 730 nm (120,000 $M^{-1}cm^{-1}$ at the 730-nm Q_y maximum) and for the 31mer(–14Cys) at 289 nm (10,200 $M^{-1}cm^{-1}$), the material in the peak at 60 min exhibited a 1:1 ratio of **BC2**:polypeptide.

FTIR spectroscopy. The FTIR spectra of the peptides were collected at room temperature on solid films deposited on a Au substrate (200 nm Au atop a 20 nm Cr adhesion layer on a Si substrate). The films were prepared by depositing 50 µL of the peptide in solution (either DMF or DMSO/CH_2Cl_2 (1:1)) onto the substrate contained in a sealed vial under Ar. The

deposited droplet was then allowed to sit on the substrate for times varying from 10 min to 15 h after which the substrate was washed three times with CH_2Cl_2 and dried under a stream of Ar.

The FTIR spectrometer was a Bruker Tensor 27 equipped with a Harrick Scientific Ge attenuated total reflection accessory (GATR™, 65° incidence angle relative to the surface normal). The substrates were placed in contact with the flat surface of a semispherical Ge crystal that serves as the optical element. The IR spectra were collected with *p*-polarized light using a liquid-nitrogen cooled medium-bandwidth (600–4000 cm^{-1}) MCT detector, averaging over 256 scans; the spectral resolution was 4 cm^{-1}. The spectra of the films were referenced against a bare Au substrate. The Ge crystal was cleaned with neat 2-butanone before every experiment, and the GATR™ accessory was purged with dry N_2 during data acquisition.

Ellipsometry. Ellipsometric measurements on the peptide films (prepared as described above) were carried out on a Jobin-Yvon Uvisel Model M200 phase modulated bench top unit using a Xenon lamp as the light source (maximum intensity at 450 nm). The incident angle was fixed at 70° and the wavelength was changed from 300 nm to 800 nm in 5-nm increments. The ellipsometric parameters were fitted using the Levenberg-Marquardt regression method. The film thickness was calculated using a modified polyimide model wherein the values of the refractive index ranged from 1.45 to 1.50.[S1]

Static and time-resolved optical spectroscopy. Static absorption measurements employed a Varian Cary 50 or 100 or Shimadzu UV-1800 spectrometer. Static fluorescence measurements employed a Spex Fluorolog Tau 2 or PTI Quantamaster 40 spectrofluorometer. Fluorescence lifetimes were obtained via decay measurements using a Photon Technology International LaserStrobe TM-3, composed of a GL-3300 nitrogen laser with a GL-302 dye laser unit and time-correlate-single-photon-counting detection. The apparatus has an approximately Gaussian instrument response function with a full-width-at-half-maximum of ~1 ns. Excitation pulses were provided by the nitrogen-pumped dye laser (350-650 nm). Static emission measurements employed 0.2-nm data intervals and typical monochromator bandwidths of 2–4 nm. Most measurements (500 nm to ≥1100 nm) utilized a setup consisting of an InGaAs detector with lock-in detection and excitation light chopped at 30 Hz; the detection monochromator bandwidth was increased to up to 8 nm for some measurements of weak B820 NIR emission. Some experiments (450–850 nm) utilized a setup containing a Hamamatsu R928 photomultiplier tube. For both setups, emission spectra were corrected for detection-system spectral response. The fluorescence yield determinations, depending on the absorption and emission wavelengths involved, employed a number of different standards whose yields were cross-checked with respect to each other. These standards were (1) free base *meso*-tetraphenylporphyrin (**FbTPP**) in nondegassed toluene, for which $\Phi_f = 0.070$ was established with respect to the zinc chelate **ZnTPP** in nondegassed toluene ($\Phi_f = 0.030$),[S2] consistent with prior results on **FbTPP**,[S3] and (2) 8,8,18,18-tetramethylbacteriochlorin[15] in Argon-purged toluene, for which $\Phi_f = 0.14$ was established with respect to **FbTPP** and chlorophyll *a* (**Chl *a***) in deoxygenated benzene[S4] or toluene[S5] (both with $\Phi_f = 0.325$). Measurements of fluorescence spectra, fluorescence excitation spectra, fluorescence quantum yields, and fluorescence lifetimes employed samples having an absorbance (A) ≤ 0.1 at the excitation wavelength(s). Under these conditions, the pertinent regions (e.g., 450-650 nm) of the absorption and absorptance spectra have the same shapes; the latter spectrum is the most relevant for quantitative comparisons with the excitation spectra to estimate the energy-transfer efficiencies in the biohybrid complexes. Samples of **OGR** and **RR** (in 1:1 DMF/Tris-buffer and phosphate buffer, respectively) and **BC1** and **BC2** (in toluene) were typically purged (bubbled) with argon in septum-stoppered cuvettes.

Samples of the peptide-bound chromophores and biohybrid complexes in detergent solutions were typically purged by passing Argon over the stirred solution.

Time-resolved pump-probe absorption experiments were carried out using a Helios femtosecond transient absorption spectrometer (Ultrafast Systems) coupled to a femtosecond laser system (Newport/Spectra-Physics). The one-box Solstice amplified ultrafast laser system consists of a Mai-Tai femtosecond oscillator whose output goes to a Spitfire Pro XP regenerative amplifier that is pumped by an Empower diode-pumped solid state pulsed green laser. The amplifier produces 800 nm pulses (~3.5 mJ, ~90 fs) at 1 kHz. The output beam is split into two and used to generate (i) the pump beam (90%) in a Topas-C optical parametric amplifier (Light Conversion, Lithuania) and (ii) probe pulses (10%) for the Helios transient-absorption spectrometer. The pump (excitation) pulses pass through a depolarizer to provide isotropic excitation of the sample and avoid pump-probe polarization effects. Individual ΔA spectra are acquired using excitation light chopped at 0.5 kHz (to provide alternate accumulations of the probe light with and without excitation) and averaged over 1-5 s (typically 2 s). Final ΔA spectra represent the average of 1000 such individual spectra. For the experiments reported here, the excitation pulses (typically of energy 2 μJ/pulse) were adjusted to have a spot diameter of 1 mm. For some experiments, studies of the signal characteristics as a function of excitation-pulse energies up to 6 μJ/pulse were examined to insure that multiphoton effects were avoided at the lower energies normally used.

The samples were typically excited near the peaks of the main absorption features shown in the spectra below and in the paper. For example, for bacteriochlorin **BC2**, and the peptide or biohybrids containing that chromophore, experiments were performed that utilized excitation in either the Q_x band (~515 nm) or the Q_y band (~720 nm). Samples were contained in 2-mm or 1-cm path cuvettes and were mixed continuously using a magnetic micro-stirrer to minimize photo-degradation. Control samples consisting of a chromophore-attached peptide or biohybrid antenna complex typically had an absorbance of ≤0.15 in the main absorbance feature.

Studies of RR.

Time-resolved absorption data for **RR** in solution (Figure S-4) and biohybrid [31mer(−14Cys)RR/BChl]$_2$ and control peptide 31mer(−14Cys)RR (Figure S-5) were obtained using a 0.1 ps flash at 526 nm. The data in Figures S-4, S-5A and S-5B probe decay of RR* in the region of **RR** bleaching and RR* stimulated emission at 580 nm. The RR* decay for **RR** in buffer solution (Figure S-4) is clearly not single exponential and is described well by a dual exponential with components of 215 ps (0.24) and 1510 ps (0.76) or a triple exponential with time constants of 1 ps (0.07), 260 ps (0.24), and 1570 ps (0.69). Similarly, in Figure S-5B, a fit to the decay profile (following the instrument-limited rise) for [31mer(−14Cys)RR/BChl]$_2$ (black line) requires a triple exponential with time constants (and relative fractions) of 2.1 ps (0.41), 43 ps (0.31), and 1355 ps (0.28). The decay profile for control peptide 31mer(−14Cys)RR (red line) is also triple exponential with components of 4.1 ps (0.25), 78 ps (0.20), and 1860 ps (0.52).

The multi-phasic decay of RR* even when the dye is not appended to a peptide indicates that more than one form (conformation, etc.) is present in solution. The forms may be modified in a number of properties when **RR** is attached to the peptide in 31mer(−14Cys)RR. For example, RR* may be sensitive to different environments sampled by motion of the chromophore with respect to the peptide, some of which could slightly lengthen a lifetime component or lead to quenching interactions with amino acids. Some of the same locales would be sampled by **RR** in [31mer(−14Cys)RR/BChl]$_2$, in which energy transfer from **RR** to B820 provides an additional avenue for RR* decay for each form. Energy transfer no doubt underlies

the reduced time constants and increased weightings of the middle and short components for [31mer(−14Cys)RR/BChl]$_2$ versus 31mer(−14Cys)RR. The amplitude-weighted decay time constant for [31mer(−14Cys)RR/BChl]$_2$ is (2.1 ps)(0.41)+(43 ps)(0.31)+(1355 ps)(0.28) = 394 ps while that for 31mer(−14Cys)RR is (4.1 ps)(0.25)+(78 ps)(0.20)+(1860 ps)(0.52) = 984 ps. These values afford $\Phi_{ENT} = 1 - (394 \text{ ps} / 984 \text{ ps}) = 0.60$.

Additional support for energy transfer in [31mer(−14Cys)RR/BChl]$_2$ is derived from the data in Figures S5-C and D. Figure S-5C shows that following excitation of **RR** (λ_{exc} = 535 nm) energy transfer from RR* to B820 produces B820* and thus B820 Q_y bleaching and stimulated emission. Figure S-5D shows a clear lag/rise in the development of the B820 bleaching for [31mer(−14Cys)RR/BChl]$_2$ (black) compared to the instrument-limited rise observed for direct excitation (λ_{exc} = 590 nm) of B820 in [31mer(−14Cys)BChl]$_2$ (blue). The development of B820* in the biohybrid has a time constant of ~5 ps, although good fits are obtained with a rise time in the range 3–8 ps. This lag can be associated with the fast components to the RR* decay (and thus energy transfer) convolved with the fast components of the B820* dynamics expected from the time profile for B820* in the absence of **RR** in [31mer(−14Cys)BChl]$_2$, which minimally includes 3 ps relaxation and 50 ps decay components (Figure S5-D). The slower phase(s) of B820* decay extending to hundreds of picoseconds for [31mer(−14Cys)RR/BChl]$_2$ are also consistent with the inherent 600 ps B820* decay component observed in [31mer(−14Cys)BChl]$_2$. Thus, the overall B820* time profile in the biohybrid complex is reasonably understood considering the inherent multi-component decays of the donor and acceptor even in the absence of each other.

Analogous time-resolved absorption studies of the RR* decay profile via Q_y bleaching were performed on oligomeric subunit complex [31mer(-14Cys)RR/BChl]$_n$ (Figure S-7). The RR* decay time constants (and relative amplitudes) of 1.3 ps (0.65), 20 ps (0.24), and 583 ps (0.11) for oligomer [31mer(-14Cys)RR/BChl]$_n$ and 4.1 ps (0.25), 78 ps (0.23), and 1860 ps (0.52) for control peptide 31mer(−14Cys)RR; comparison of the amplitude-weighted average lifetimes gives $\Phi_{ENT} = 100[1 - (70 \text{ ps} / 984 \text{ ps})] = 0.93$.

Time-resolved NIR absorption measurements on the B850 Q_y bleaching of [31mer(−14Cys)RR/BChl]$_n$ (Figure S-7D) show a non-instrument limited ~1 ps rise consistent with the 1.3 ps component of RR* decay followed by decay components of 10 and 40 ps of comparable amplitude and a minor (10%) phase lasting several hundred picoseconds.. The latter are consistent with a convolution of the slower component of RR* decay and the inherent B850* decay components measured in control oligomer [31mer(−14Cys)BChl]$_n$ (Figure 8).

Förster Calculations

[a]The energy-transfer efficiency (Φ_{ENT}) for each of the biohybrid ββ-subunit complexes [31mer(−14Cys)X/BChl]$_2$ (X = **OGR**, **RR**, **BC1**, **BC2**) and [31mer(−6Cys)OGR/BChl]$_2$ was calculated using PhotochemCad.[42] The calculations use the "R_0 method" in which R_0 is the distance at when the efficiency is 50%. The expression for the energy-transfer efficiency is $\Phi_{ENT} = R_0^6 / (R^6 + R_0^6)$, where $R_0^6 = (8.8 \times 10^{23}) \kappa^2 \Phi_f J n^{-4}$. (See the PhotochemCad documentation for the development of the expression.) Here, n is solvent refractive index; κ^2 is the orientation term for which the dynamically averaged value of 1.125 was used; R is the center to center (in Å) distance of the energy-donor chromophore and the BChl-*a* acceptor complex B820; Φ_f is the fluorescence quantum yield of the chromophore in the absence of the acceptor (given in Table 1 of the manuscript); J is the spectral overlap integral and is calculated using the emission spectrum of the control peptide 31mer(−14Cys)X that contains chromophore X and the

absorption spectrum of the BChl-*a* dimer B820 in the synthetic chromophore-free complex $[31mer(-14Cys)BChl]_2$, for which the molar absorptivity at 820 nm is ε = 172,000 $M^{-1}cm^{-1}$. Note that the equation used in the calculation does not use the lifetime of the donor chromophore in either the absence or presence of the acceptor. This is advantageous if one does not know the lifetime, or when the excited-state decay profile is multi-exponential, as it is for **RR** even in solution and not attached to the 31mer peptide (both in the absence of acceptor).

References

(1) Blankenship, R. E.; Tiede, D. M.; Barber, J.; Brudvig, G. W.; Fleming, G.; Ghirardi, M.; Gunner, M. R.; Junge, W.; Kramer, D. M.; Melis, A.; Moore, T. A.; Moser, C. C.; Nocera, D. G.; Nozik, A. J.; Ort, D. R.; Parson, W. W.; Prince, R. C.; Sayre, R. T. *Science* **2011**, *332*, 805–809.

(S1) Vörös, J. *Biophys. J.* **2004**, *87*, 553–561.

(S2) Seybold, P. G.; Gouterman, M. *J. Mol. Spectrosc.* **1969**, *31*, 1–13.

(S3) Gradyushko, A. T.; Sevchenko, A. N.; Solovyov, K. N.; Tsvirko, M. P. *Photochem. Photobiol.* **1970**, *11*, 387–400.

(S4) Weber, G.; Teale, F. W. J. *Trans. Faraday Soc.* **1957**, *53*, 646–655.

(S5) Mass, O.; Taniguchi, M.; Ptaszek, M.; Springer, J. W.; Faries, K. M.; Diers, J. R.; Bocian, D. F.; Holten, D.; Lindsey, J. S. *New J. Chem.* **2011**, *35*, 76–88.

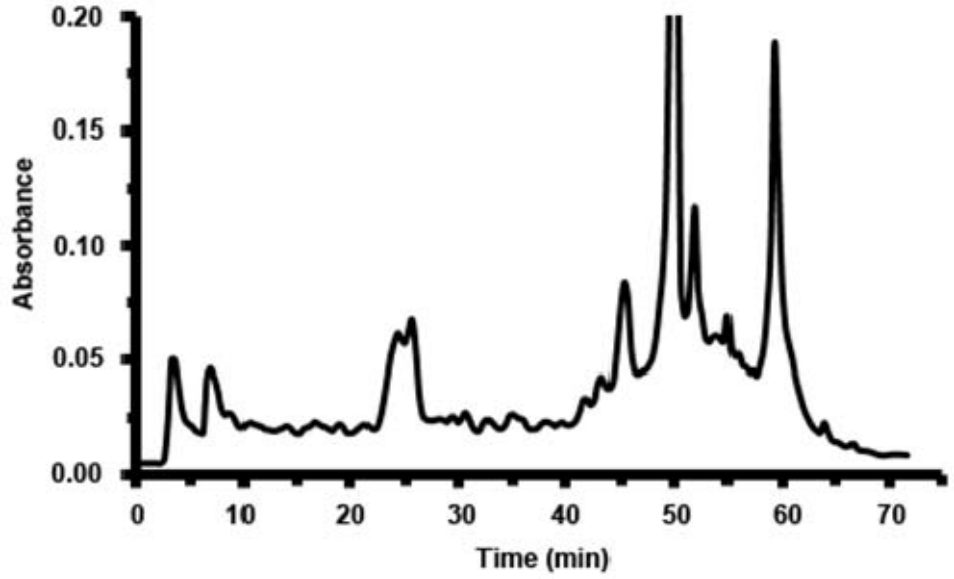

Figure S-1. HPLC chromatogram of 31mer(−14Cys)BC2 (λ_{det} = 280 nm). The peak at 60 min is the 31mer(−14Cys)BC2 product and that at 50 min is free **BC2**. (For some preparations, the dried sample was first extracted twice with methanol to remove free **BC2**, dried under a stream of Argon and then dried overnight under vacuum. Subsequent HPLC analysis showed little free **BC2**.) Fractions of the 60-min peak were cut and collected to give the sample of 31mer(−14Cys)BC2 that was examined in the spectroscopic studies described herein.

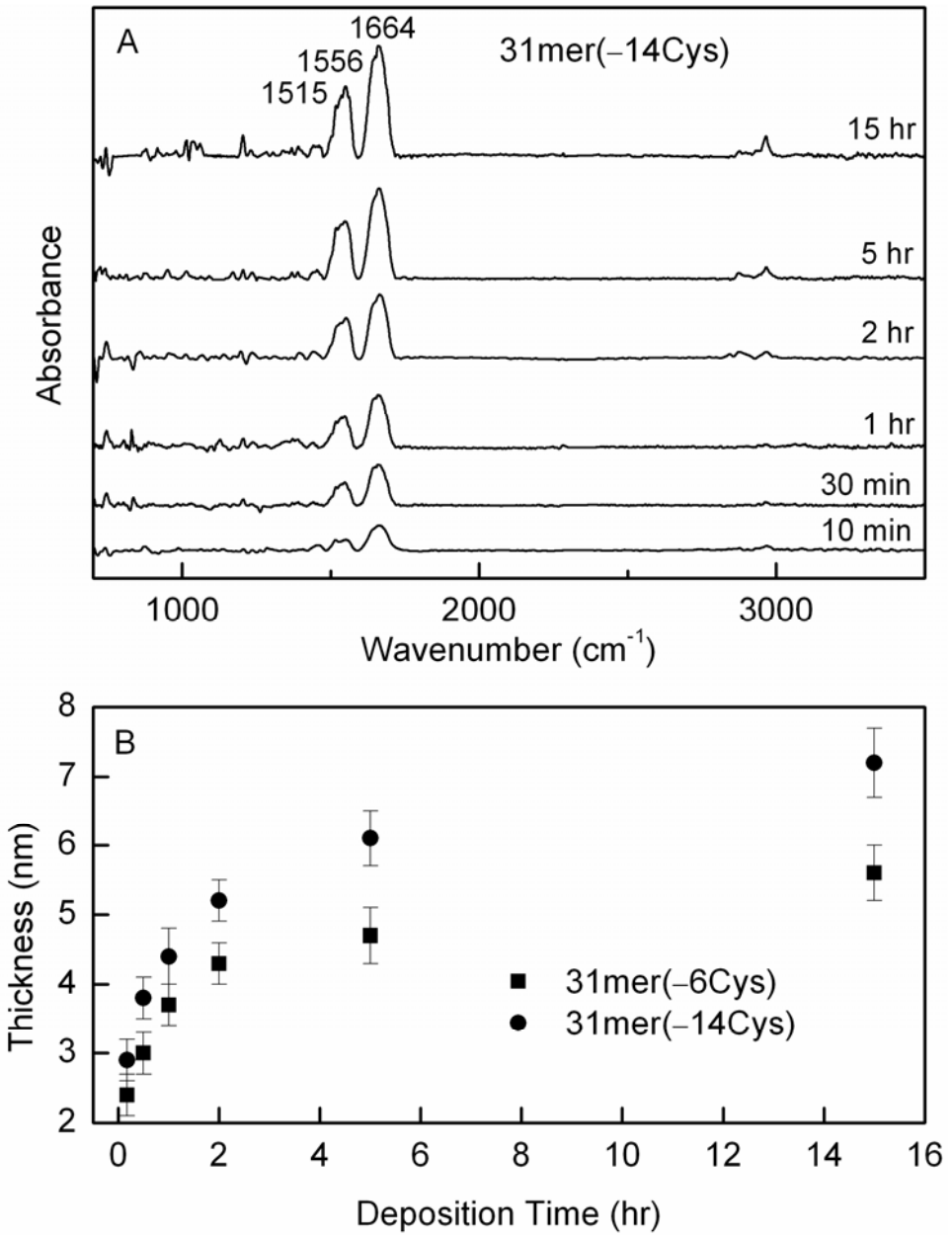

Figure S-2. (A) Single-reflection infrared data for films of peptides as a function of deposition time: (A) spectra of 31mer(–14Cys) and (B) thickness of films of 31-mer(–14Cys) (circles) and 31-mer(–6Cys) (squares).

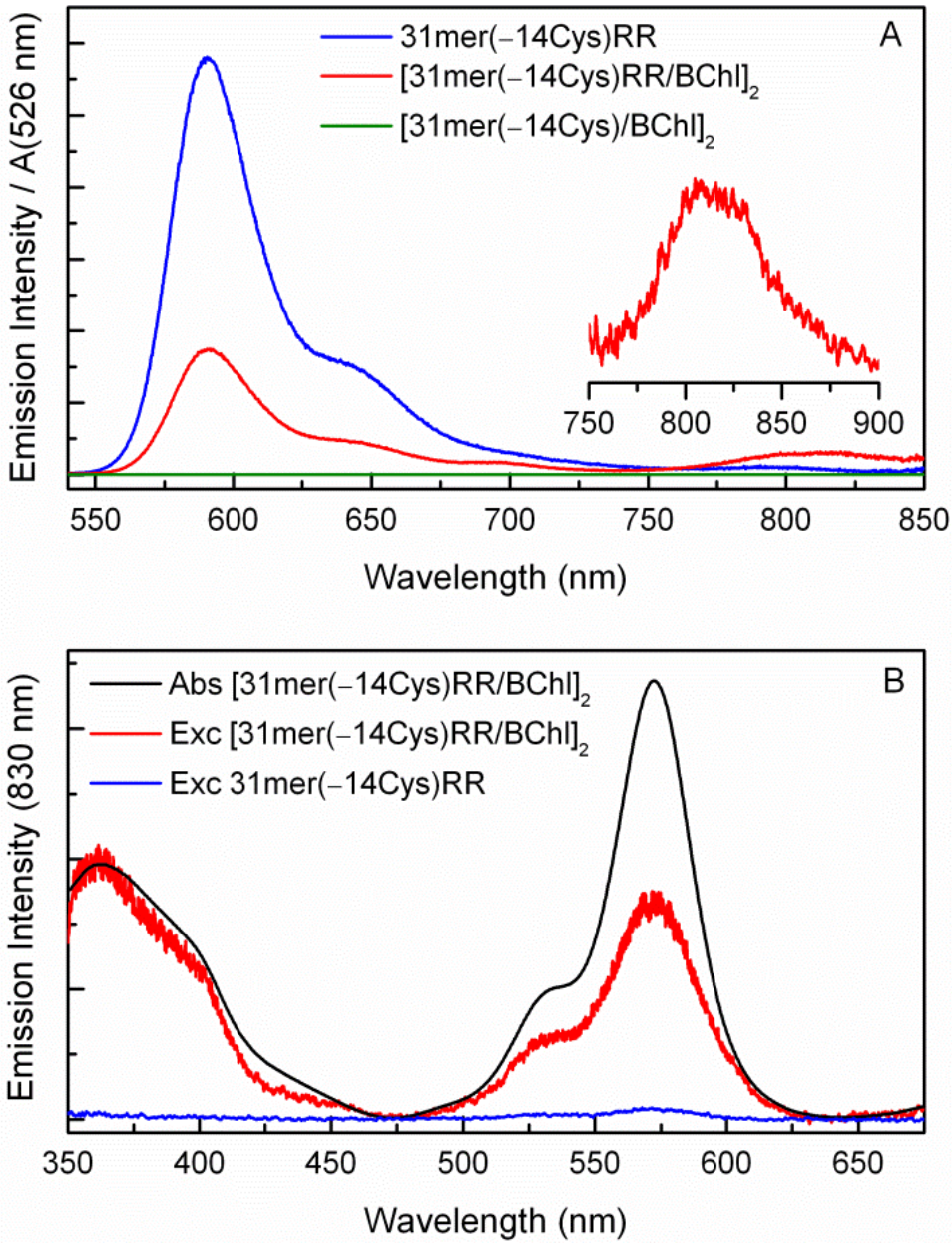

Figure S-3. (A) Fluorescence spectra (λ_{exc} = 526 nm) for peptide 31mer(–14Cys)RR (blue) and complexes [31mer(–14Cys)RR/BChl]$_2$ (red) and [31mer(–14Cys)BChl]$_2$ (green). The intensities are divided by the absorbance at λ_{exc} = 526 nm for (A) and 830 nm for (B). The inset shows the emission spectrum of [31mer(–14Cys)RR/BChl]$_2$ obtained using a NIR-enhanced detection system. (B) Fluorescence excitation spectrum for [31mer(–14Cys)RR/BChl]$_2$ (λ_{det} = 830 nm) (red) normalized to the absorption spectrum at 365 nm (black). Fluorescence excitation spectrum for 31mer(–14Cys)RR (λ_{det} = 830 nm) (blue) scaled by the **RR** fluorescence yield relative to that for [31mer(–14Cys)RR/BChl]$_2$.

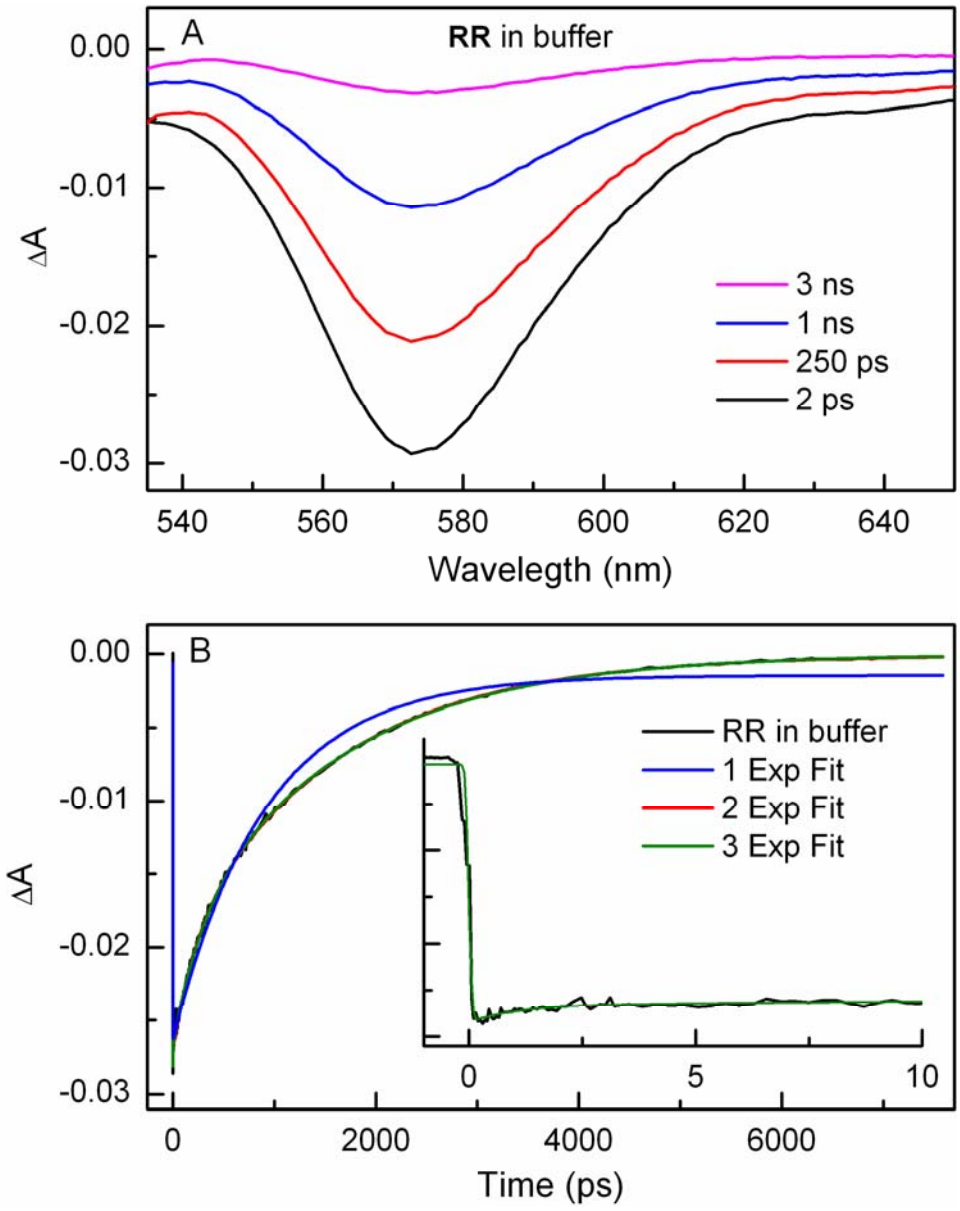

Figure S-4. Time-resolved absorption data using λ_{exc} = 535 nm for **RR** in 100 mM phosphate buffer (pH 7.5). Panel (A) gives spectra and panel (B) shows a kinetic trace at 580 nm (black) and fits to a single- (blue), double- (red) or triple (green) exponential.

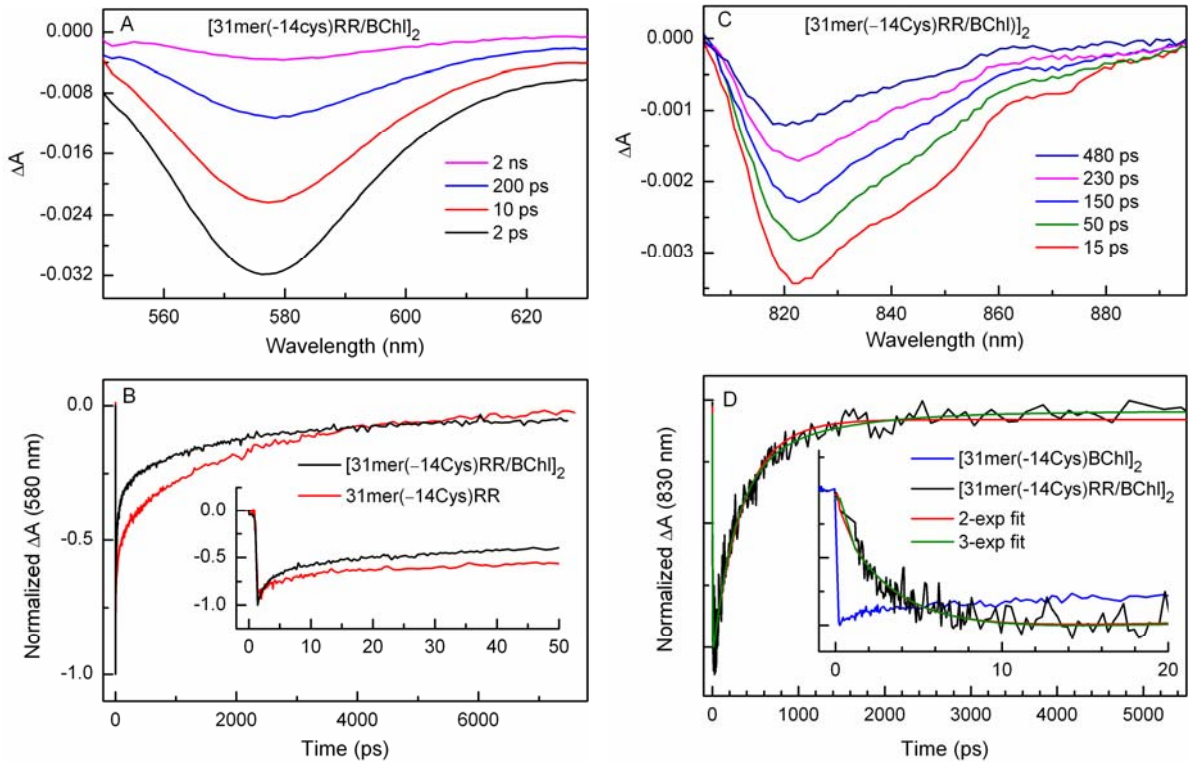

Figure S-5. Time-resolved absorption data for [31mer(–14Cys)RR/BChl]$_2$ in the Q_y region using λ_{exc} = 535 nm. Panel (A) shows combined bleaching and stimulated emission for **RR** and panel (C) for B820 (C). Panel (B) shows a kinetic traces at 580 nm for RR and panel (D) for B820 at 830 nm for [31mer(–14Cys)RR/BChl]$_2$ (black), 31mer(–14Cys)RR (red), and [31mer(–14Cys)BChl]$_2$ (blue) Panel D (lower right) shows dual- (red) and triple- (green) exponential function for [31mer(–14Cys)RR/BChl]$_2$.

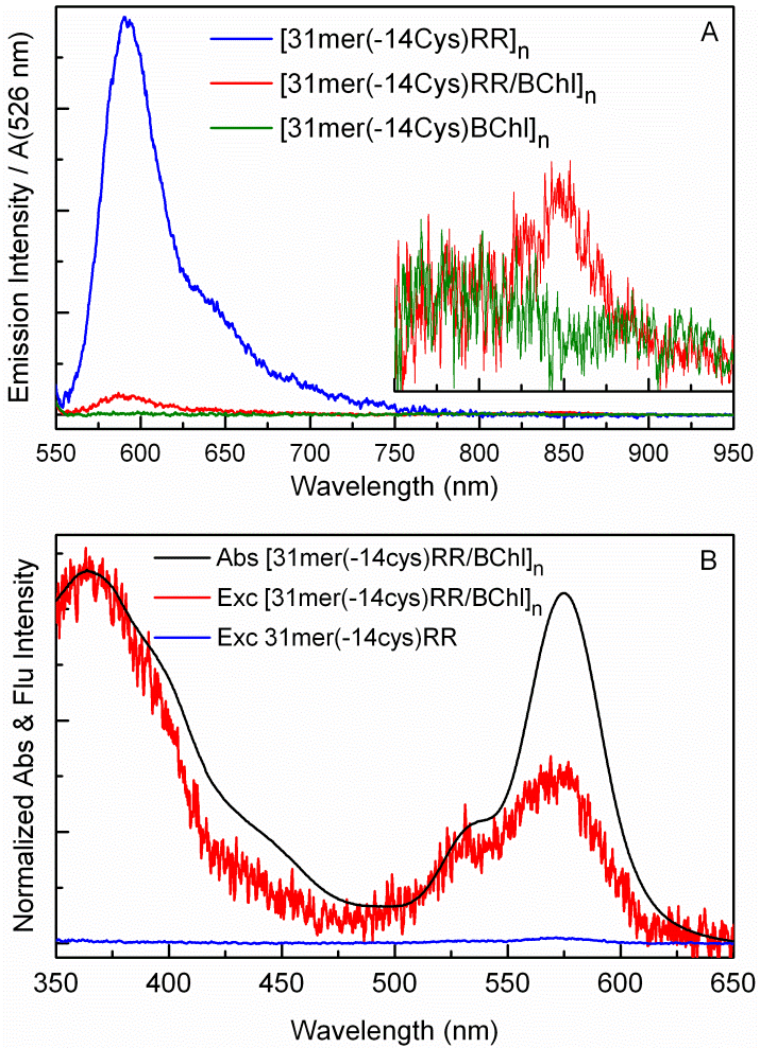

Figure S-6. (A) Fluorescence spectra (λ_{exc} = 526 nm) for 31mer(–14Cys)RR (blue), [31mer(–14Cys)RR/BChl]$_n$ (red) and [31mer(–14Cys)BChl]$_n$ (green). The intensities are divided by the absorbance at λ_{exc} = 526 nm. The inset shows the spectrum of [31mer(–14Cys)RR/BChl]$_n$ for the same sample and λ_{exc} with a red-enhanced detection system. (B) Fluorescence excitation spectrum (λ_{det} = 850 nm) for [31mer(–14Cys)RR/BChl]$_n$ (red) and 31mer(–14Cys)RR (blue), with the latter scaled by the **RR** fluorescence yield relative to that for [31mer(–14Cys)RR/BChl]$_n$. The absorption spectrum (black) and excitation spectrum of [31mer(–14Cys)RR/BChl]$_n$ are normalized at 365 nm.

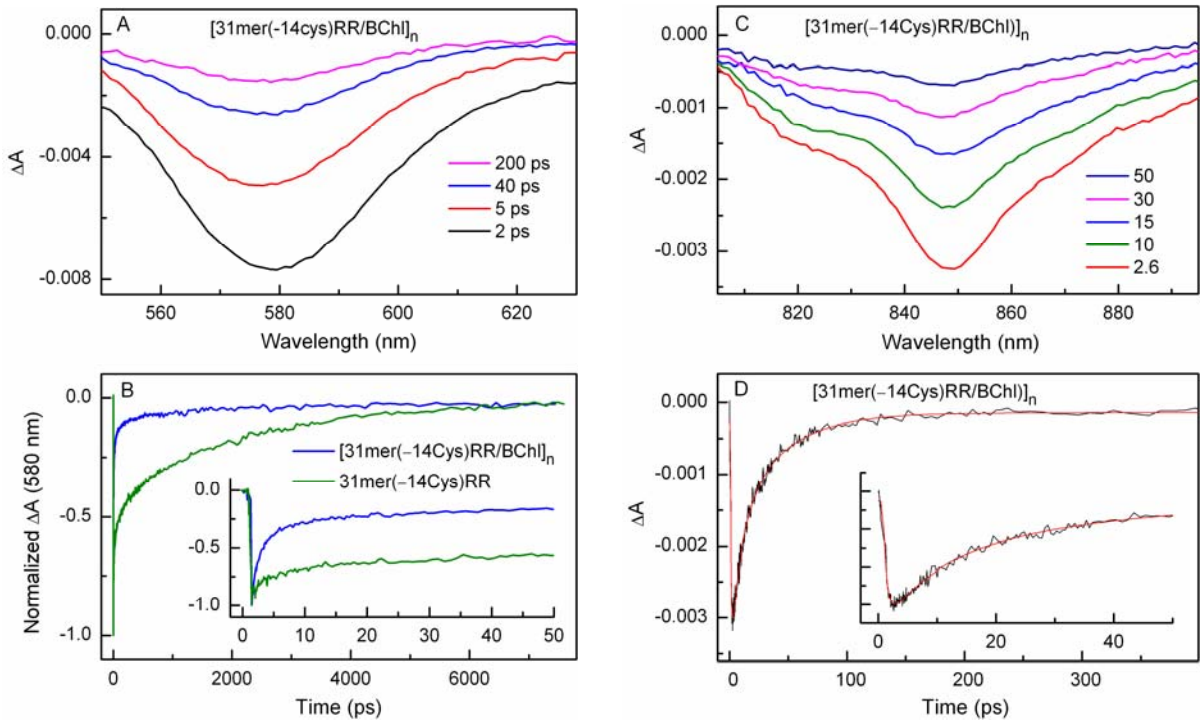

Figure S-7. (A) Time-resolved absorption spectra for $[31mer(–14Cys)RR/BChl]_n$ and (B) kinetic traces at 580 nm for $[31mer(–14Cys)RR/BChl]_n$ (blue) and 31mer(–14Cys)RR (green) using λ_{exc} = 535 nm. (C) Time-resolved absorption spectra for $[31mer(–14Cys)RR/BChl]_n$ and (D) kinetic trace at 850 nm and a fit to a triple-exponential function using λ_{exc} = 535 nm.

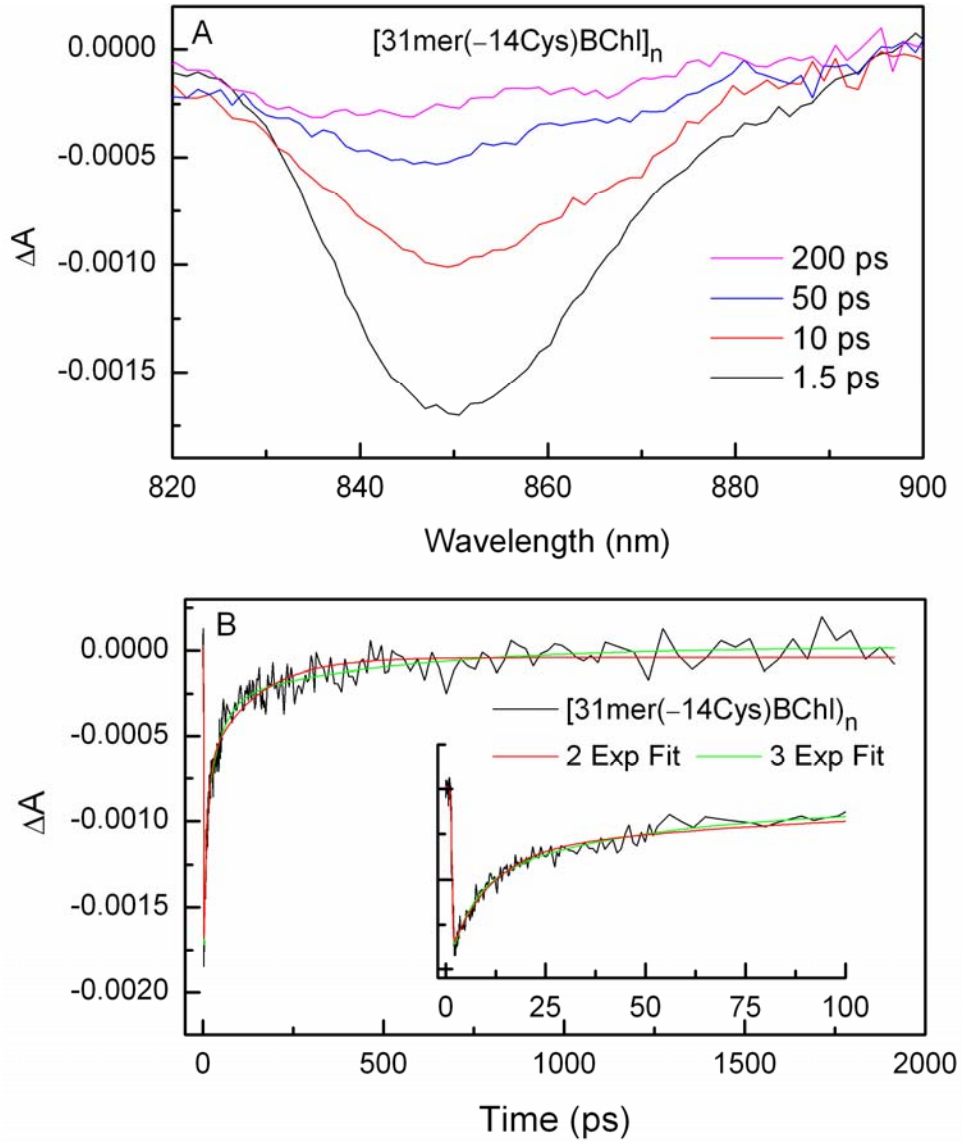

Figure S-8. (A) Time-resolved absorption spectra and (B) kinetic trace at 850 nm (black) and fits to two exponentials (red) and three exponentials (green) for [31mer(–14Cys)BChl]$_n$ (λ_{exc} = 590 nm) at room temperature.

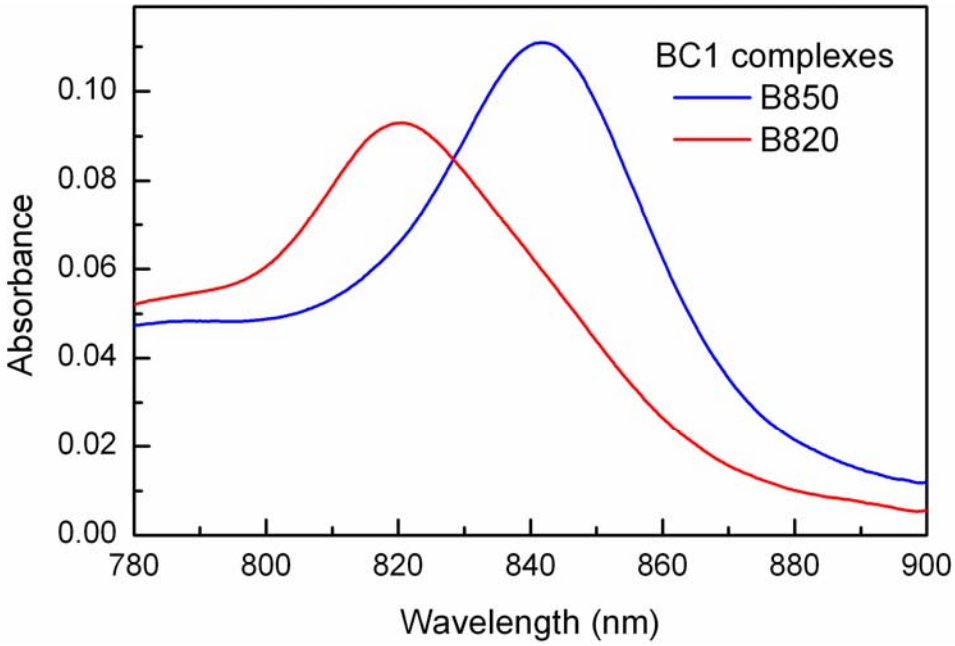

Figure S-9. NIR absorption spectra of oligomeric complex $[31mer(-14cys)BC1/BChl]_n$ (0.66% octyl glucoside solution) at room temperature (blue) and ββ-subunit complex $[31mer(-14cys)BC1/BChl]_2$ obtained by heating the solution of the oligomeric complex at 39 °C (red).

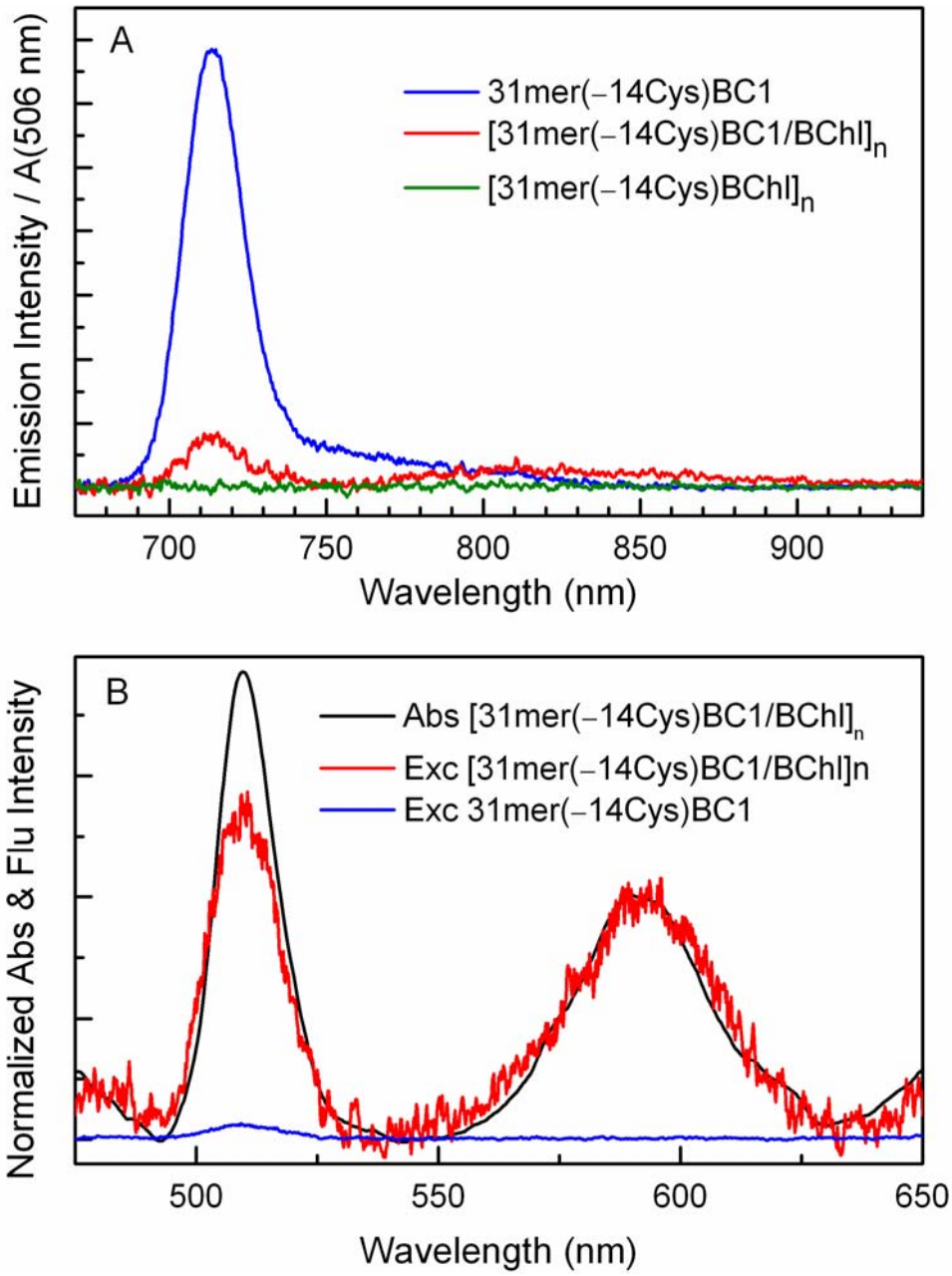

Figure S-10. (A) Fluorescence spectra (λ_{exc} = 506 nm) for peptide 31mer(–14Cys)BC1 (blue) and complexes [31mer(–14Cys)BC1/BChl]$_n$ (red) and [31mer(–14Cys)BChl]$_n$ (green). The intensities are divided by the absorbance at λ_{exc} – 506 nm. (B) Fluorescence excitation spectrum for [31mer(–14Cys)BC1/BChl]$_n$ (λ_{det} = 850 nm) (red) normalized to the absorption spectrum at 590 nm (black). Fluorescence excitation spectrum for 31mer(–14Cys)BC1 (λ_{det} = 850 nm) (blue scaled by the BC1 fluorescence yield relative to that for [31mer(–14Cys)BC1/BChl]$_n$.

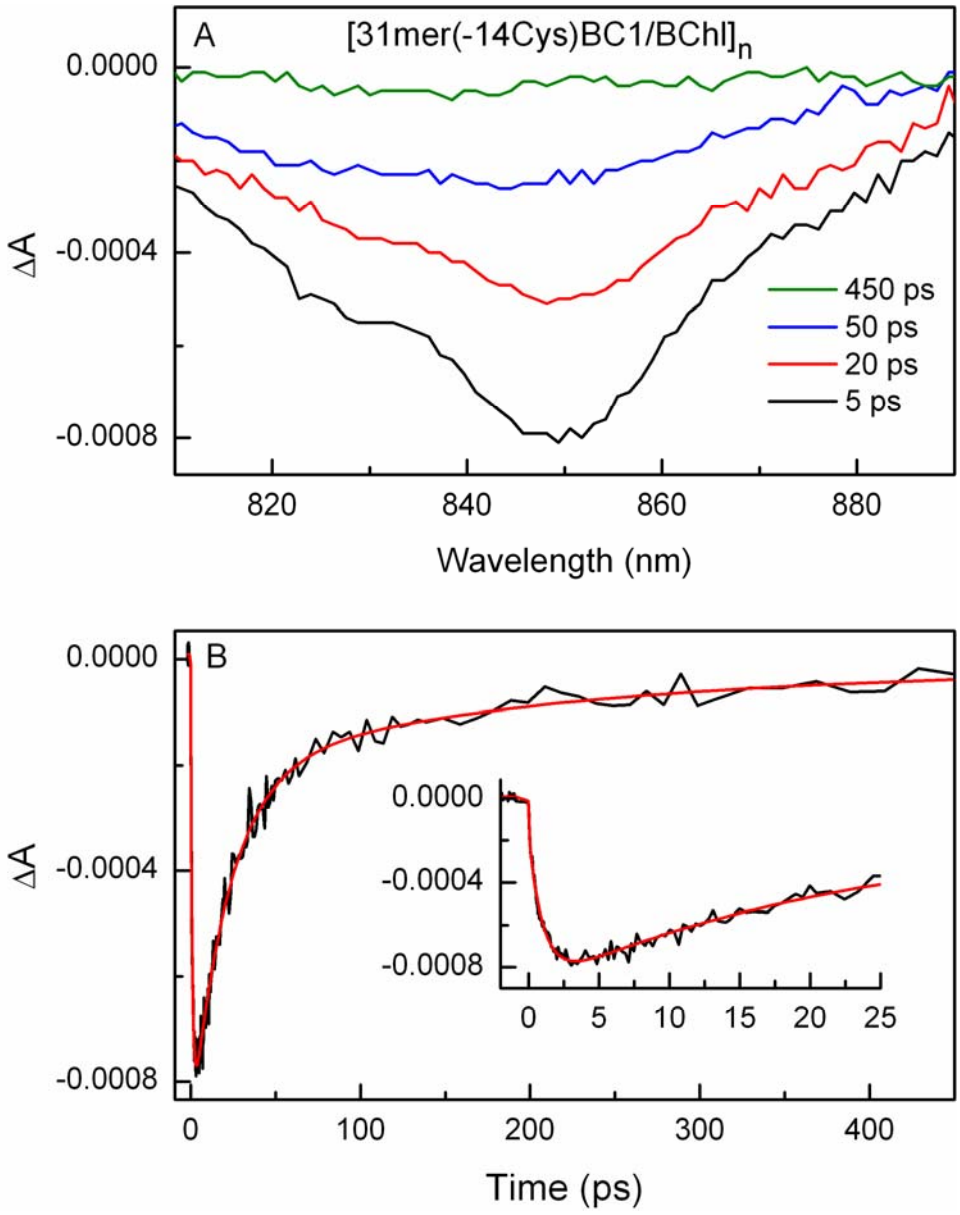

Figure S-11. (A) Time-resolved absorption spectra and (B) kinetic trace at 850 nm (black) and a fit to three exponentials (red) for $[31mer(-14Cys)BC1/BChl]_n$ (λ_{exc} = 506 nm) at room temperature.

MOLECULAR PROBES®

CERTIFICATE OF ANALYSIS

Catalog Number	R6160
Product Name	Rhodamine Red™-X, succinimidyl ester *5-isomer*
Molecular Formula	$C_{37}H_{44}N_4O_{10}S_2$
Molecular Weight	768.9
Appearance	red solid
Lot Number	792626

	LOT DATA	SPECIFICATION
Absorption[1]		
Maximum	560 nm	560 ± 3 nm
Extinction	120000 $cm^{-1}M^{-1}$	126000 ± 9000 $cm^{-1}M^{-1}$
Fluorescence[1]		
Emission Maximum	581 nm	580 ± 4 nm
HPLC[2]		
Purity	97 % at 254 nm	≥ 90 % at 254 nm
NMR		
Result	meets specification	consistent with structure
Miscellaneous Information		
Material Lot Number	774604	N/A

1. Solvent: Methanol.

2. Method: Derivatized with n-butylamine. Purity value represents total reactive dye content.

Terence Featherstone, Ph.D., Biosciences Quality Control Manager

21-Jun-2010

Life Technologies Corporation, on behalf of its Invitrogen business, Molecular Probes® labeling and detection technologies, certifies on the date above that this is an accurate record of the analysis of the subject lot and that the data conform to the specifications in effect for this product at the time of analysis.

Molecular Probes, Inc.
29851 Willow Creek Road
Eugene, OR 97402-9132
Phone (541) 465-8300 Fax (541) 335-0504

Printed Oct 14, 2011

MOLECULAR PROBES®

CERTIFICATE OF ANALYSIS

Catalog Number	O6010
Product Name	Oregon Green® 488 iodoacetamide *mixed isomers*
Molecular Formula	$C_{22}H_{12}F_2INO_6$
Molecular Weight	551.24
Appearance	orange solid
Lot Number	795792

	LOT DATA	SPECIFICATION
Absorption[1]		
Maximum	492 nm	491 ± 3 nm
Extinction	80800 $cm^{-1}M^{-1}$	77000 ± 5500 $cm^{-1}M^{-1}$
Fluorescence[1]		
Emission Maximum	516 nm	516 ± 4 nm
HPLC[2]		
Purity	97 % at 254 nm	≥ 85 % at 254 nm
NMR		
Result	meets specification	consistent with structure
Miscellaneous Information		
Material Lot Number	33298	N/A

1. Solvent: Buffer, 50 mM potassium phosphate (pH 9).

2. Method: Purity value represents summation of the areas of individual isomers.

Terence Featherstone, Ph.D., Biosciences Quality Control Manager

14-Dec-2005

Life Technologies Corporation, on behalf of its Invitrogen business, Molecular Probes® labeling and detection technologies, certifies on the date above that this is an accurate record of the analysis of the subject lot and that the data conform to the specifications in effect for this product at the time of analysis.

Molecular Probes, Inc.
29851 Willow Creek Road
Eugene, OR 97402-9132
Phone (541) 465-8300 Fax (541) 335-0504

Printed Feb 10, 2011